DIRECT CONTAINMENT HEATING AT LOW PRIMARY PRESSURE: EXPERIMENTAL INVESTIGATION AND MULTIDIMENSIONAL MODELING

Renaud Meignen[1], Delphine Plassart, Cataldo Caroli,
Institut de Radioprotection et de Sûreté Nucléaire
BP 17, 92262 Fontenay-aux-Roses, cedex, FRANCE
Phone:+33 1 5835 8579, Fax:+33 1 5835 8559, E-Mail: renaud.meignen@irsn.fr

Leonhard Meyer, Dirk Wilhelm
Forschungszentrum Karlsruhe GmbH
Postfach 3640, 76021 Karlsruhe, GERMANY
Phone:+49 7247 82 2469, Fax:+49 7247 82 6323, E-Mail: meyer@iket.fzk.de

ABSTRACT

The Direct Containment Heating (DCH) issue, in Pressurized Water Reactor (PWR) plants having a direct path from the reactor cavity to the containment dome, has been investigated for low primary pressure (less than 20 bar). In the frame of a French-German collaboration between IRSN and FZK new experiments have been carried out using simulant materials and 3-dimensional high geometrically detailed mock-ups of the French P'4 plant at the linear scale 1/16. Two series of experiments have been carried out using two separate, but geometrically similar, experimental installations: 1) The "Cold" experiments focus on the corium entrainment and dispersion; 2) The "Hot" experiments give further insight of heat exchanges, and induced hydrogen combustion. Among the investigated conditions the case of an inert initial containment atmosphere has been considered and was funded by the EU Commission (LACOMERA project). Results of this test and of a series of "cold" tests are presented in the paper. Beside the experimental tests, a modeling work is being carried out using the multi-dimensional multi-phase computational fluid dynamic codes AFDM and MC3D. AFDM capabilities allow complete calculations, including combustion. Pre-tests analyses have been carried out in order to better define the tests conditions and to advance the credibility of AFDM results for future extrapolations to reactor conditions, and post-test analyses to contribute to the interpretation of the experimental results. MC3D is currently used in a different way, in order to investigate details of the fuel flow characteristics.

1. INTRODUCTION

DCH phenomena have been extensively investigated between 1986 and 1998 for reactors of US-design (Zion and Surry), which are characterized by a large instrumentation tunnel connecting the reactor pit with relatively small compartments (Pilch, 1996). A few experiments were performed for a cavity without such connection (Blanchat, 1997), (de Bertodano, 1996). One important conclusion of these investigations was that melt dispersion and pressure build up in the containment are extremely dependent on the reactor cavity geometry, most important are the flow paths out of the lower pit.

[1] Corresponding authors

Investigations for the French 900 MWe reactor were performed at KAERI, on behalf of IRSN, with cold simulants (Kim, 1999). The reactor pit of these plants has a large exit area directly connected to the containment through the annular space around the pressure vessel. The reactor pit is also connected with a separate compartment through a large ventilation duct.

In 1998 a program was started to investigate the DCH issue for the European Pressurized Reactor (EPR) and German reactor designs. They are characterized by a narrow reactor pit without exit except through the annular space between pressure vessel and cavity wall, leading either directly to the upper containment or into the pump and steam generator rooms along the flow path around the main cooling lines. Two test facilities were built at Forschungszentrum Karlsruhe (FZK). The facility DISCO-C is suited for the investigation of fluid dynamic phenomena, such as the two-phase jet, liquid fragmentation, liquid film formation at walls, entrainment and trapping of liquid, and liquid dispersion and deposition (Meyer, 2003). In the other facility, DISCO-H, integral tests can be performed including all relevant DCH phenomena (Meyer, 2004). Both facilities can model specific reactor geometries in sufficient detail, to take account of the geometry dependence of the processes.

The interpretation of these experiments showed that the containment pressurization is mostly due to hydrogen combustion and to the heat exchanges between the fragmented corium and the containment gas. This latter phenomenon depends on the time during which corium particles and the gas evacuated from the pit are in contact (coherence). These principles are adopted in numerical DCH codes. Currently, we can distinguish two types of DCH codes: Lumped parametric models, as the DCH modules of MAAP-4, MELCOR and ASTEC (RUPUICUV), and more "mechanistic" models as used in the CONTAIN code. The lumped parametric models are based on the following hypotheses: the steam ejection from the reactor vessel takes place after the entire corium ejection following an adiabatic or isothermal expansion; the particles in suspension in the cavity and the gas are in thermal and chemical equilibrium; only a mixture of steam and hydrogen can enter into the containment in thermal balance. However, various more or less parametric correlations are used for the calculation of the corium fraction dispersed in the containment. These codes are mainly validated on tests carried out with prototypic corium or simulant materials in a mock-up at different scales of power plants. Most of the parameters of these models are very dependent on the type of the geometry and the simulant of corium.

One of the objectives of the present program is to improve the DCH ASTEC module (Cranga, 2003), suited for the French geometry. The program is divided into four parts. The experimental one takes advantage of the existing DISCO facility and French-German collaborations. Both DISCO facilities have been adapted to the geometry of the French P'4 reactor. In this paper, we will present the results and analysis of eight experiments with cold model fluids performed in DISCO-C and of one experiment with an iron-alumina melt performed in DISCO-H. The second part of the program consists in the interpretation of the experiments with two different CFD multiphase flow codes: AFDM (Bohl, 1992) and MC3D (Meignen, 2003, 2004). The third and fourth parts are underway and consist in respectively improving the RUPUICUV correlations and propose some extrapolations to the reactor situations. In the present paper, we will restrict our description to the status of the first two parts of the program.

2. EXPERIMENTAL PROGRAM

2.1. DISCO-Cold experiments

The DISCO-C facility has been modified to represent with high level detail the French 1300 MWe P'4 reactor pit geometry (scale 1/16) with four paths available for the corium to reach the containment: at the top of the annular space, along the primary loop and by the ventilation duct, and via the compartments.

Figure 1, left, shows schematically the RPV and reactor pit of DISCO-C, for the P'4 geometry. Different from the EPR pit, the P'4 pit is not symmetric. It has a niche and an exit to the pit bottom

access. The annular area around the RPV is smaller than in the EPR pit, but an extra flow cross section is provided by the eight flux chambers. The P'4 pit has eight holes leading into the refueling pool, which is open to the containment. Another important difference between the two reactor cavities is their height, or better the distance between RPV lower head and pit floor, which is much larger in the P'4 plants.

Figure 1, right, shows all components modeled in DISCO-C. There are eight compartments that model the pump and steam generator rooms (only one is shown). The refueling pool is an annular room around the steel cylinder that models the RCS-volume. The cavity is made of Plexiglas, which allows observation of the flow processes. An extra box is connected to the exit at the pit bottom to model the pit bottom access. All boxes and the annular room above the cavity are open to the environment, with the openings covered by a filter, for trapping any water droplets. Two sizes of round holes in the lower head were studied as failure modes. The holes are initially closed by a rupture disk. The steam simulant was nitrogen.

The experiments are conducted in the following way: the melt simulant, in this case water, is filled into the RPV through a small pipe. The pressure vessel is filled with nitrogen gas at a pressure close to the failure pressure of the disk. By opening a pneumatic valve between the pressure vessel and an auxiliary vessel, which is at a higher pressure, the pressure in the pressure vessel is increased until the rupture disk breaks. A break wire placed on the rupture disk gives a signal for the time mark t = 0 s, and the pneumatic valve is closed.

The most important measurements are pressure measurements in the RPV and in the reactor pit. During the blow down high speed and normal speed video cameras take pictures from the flow in the cavity, the compartments and the refueling pool. Timing of the different flow stages and an estimate of droplet sizes is possible. Immediately after the blow-down terminates all openings that were covered by a filter are sealed, to prevent any water to evaporate before its mass could be measured. The water distribution is determined by taking off all boxes and the cavity model and weighing them.

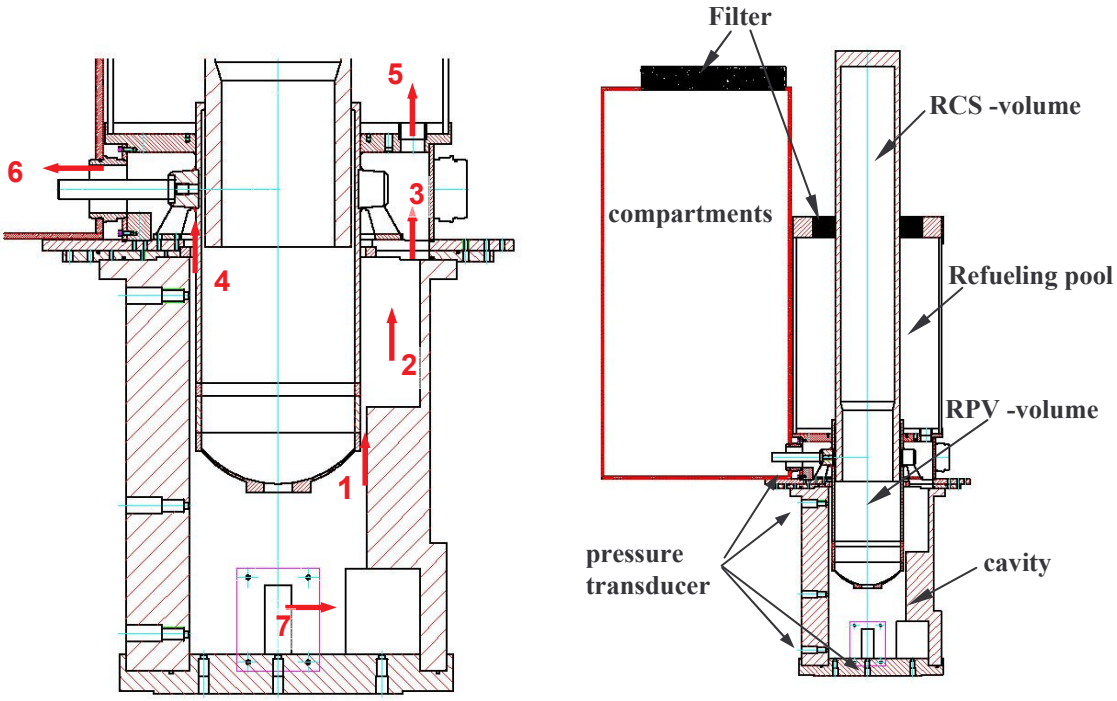

Figure 1: Scheme of the P'4 test geometry, with the flow paths out of the pit and their cross sections in (cm²): 1 annular space (109), 2 flux chambers (186), 3 exit of flux chambers (95), 4 vessel support ring (93), 5 exit to refueling pool (114), 6 primary circuit legs (395), 7 reactor pit access hatch (60)

In Table 1, the initial conditions, the timing of flow stages and the dispersed liquid fractions are listed for the first six cold experiments (F01 to F06) and one hot test, which is described later (L1). For the purpose of modeling analyses, some supplementary tests (F07 to F08) have been performed with a modified quasi-2-D geometry by just suppressing the niche and pit bottom access. Results of tests F07 and F08 are included in Table 1.

Figure 2 left, shows the blow down pressure and pressure at the pit floor just below the hole, where the jet impacts. The high pressure at the floor indicates the impact of the single phase liquid jet in the time interval 7 < t < 12 ms. The water jet needs 7 ms to reach the floor. The signal drop at 16 ms indicates the change from a compact single-phase liquid jet to a dispersed jet. In the high-speed video pictures (Fig. 3) it can be observed that the gas blow through occurs at 11.5 ms. This means that the variation of flow at the nozzle takes only 4.5 ms to reach the pit floor. The change from two-phase flow to single-phase gas flow can be determined from the change in the slope of the blow down pressure (Fig. 2 right), which occurs at 310 ms. Thus, we have a full picture of the behavior of the jet at the nozzle.

							Liquid fractions found in			
Test	**Liquid Volume [cm³]**	**Hole dia. [mm]**	**Burst pressure [MPa]**	**Blow through [ms]**	**End of 2-phase flow [ms]**	**End of Blow down [ms]**	**Pit**	**Bottom exit**	**Com-partments**	**Contain-ment**
F01	2700	30	1.124	25	350	1600	0.352	0.148	0.392	0.108
F02	2700	30	1.611	19	320	1900	0.196	0.170	0.476	0.157
F03	2700	60	1.134	4	100	480	0.233	0.206	0.419	0.142
F04	2700	60	1.624	-	-	510	0.122	0.239	0.466	0.172
F05	1800	60	1.630	3.5	60	500	0.132	0.274	0.436	0.158
F06	1800	30	1.175	12	310	1500	0.379	0.230	0.297	0.094
F07	2700	60	1.6	8	90	510	0.094	-	0.653	0.253
F08	2700	30	1.64	19	320	2000	0.117	-	0.619	0.264
L1	***2680***	***60***	***1.920***	***92***	***230***	***449***	***0.394***	***0.181***	***0.280***	***0.145***

Table 1: Parameters and liquid fractions of 7 cold and one hot experiment. F07 is done with a modified symmetrical geometry; its initial conditions are similar to F04. Test L1 is discussed later.

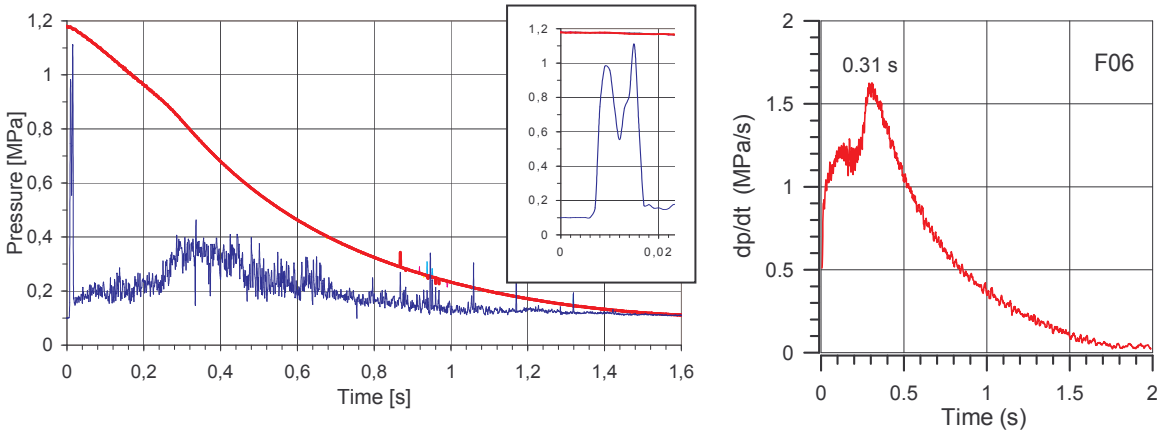

Figure 2: Left : Blow down pressure (red) and total pressure at the pit floor (blue), of test F06;
Right : Pressure gradient of blow down pressure

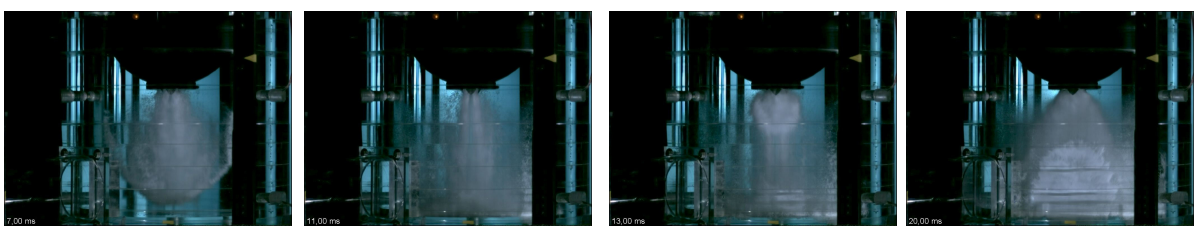

t = 7 ms t = 11 ms t = 13 ms t = 20 ms

Figure 3: Stages of the jet in test F06: t < 11.5 ms, single phase liquid; 11.5 < t < 310 ms, two-phase

Figure 4 shows a graphical representation of the dispersed fractions of all experiments including the hot test L1 (see below) and comparable tests performed earlier in EPR geometry. They compare to F01 and F03 respectively, in respect to burst pressure and hole size. The amount of water that remains in the pit is similar for both geometries. However, the ejected fraction is distributed into the three different locations available in the P'4 geometry.

The results from the hot test L1 should be compared to test F04, since the burst pressure, hole size and liquid volume were similar. However, the distribution of the melt, respectively water, is rather different. The distribution of the hot test is similar to F06, which was different in all three parameters, smaller hole size, lower pressure and less liquid volume. Apart from the temperature, the main difference between the cold and hot tests is of course the different density of the model fluids. The average density of the melt is 3878 kg/m³ versus 1000 kg/m³ for water. According to these partial results, the role of density seems quite clear and the higher the density, the lower the ejected fraction. It is clear that water is not representative of the reactor material, and results should not be extrapolated. This is why next cold tests are planned with a liquid metal as simulant (gallium).

From the first six cold experiments we can draw the following conclusions:
A similar fraction of liquid is ejected out of the pit as in the EPR geometry, but it is divided into three parts; the largest fraction goes to the reactor compartments along the main cooling lines, 15 – 27% goes to the pit bottom access and 9 to 17% is ejected into the refueling pool and from there directly into the containment dome. The effect on the distribution of the initial amount of melt is small, and is almost negligible for large holes and high pressure (F04 versus F05).

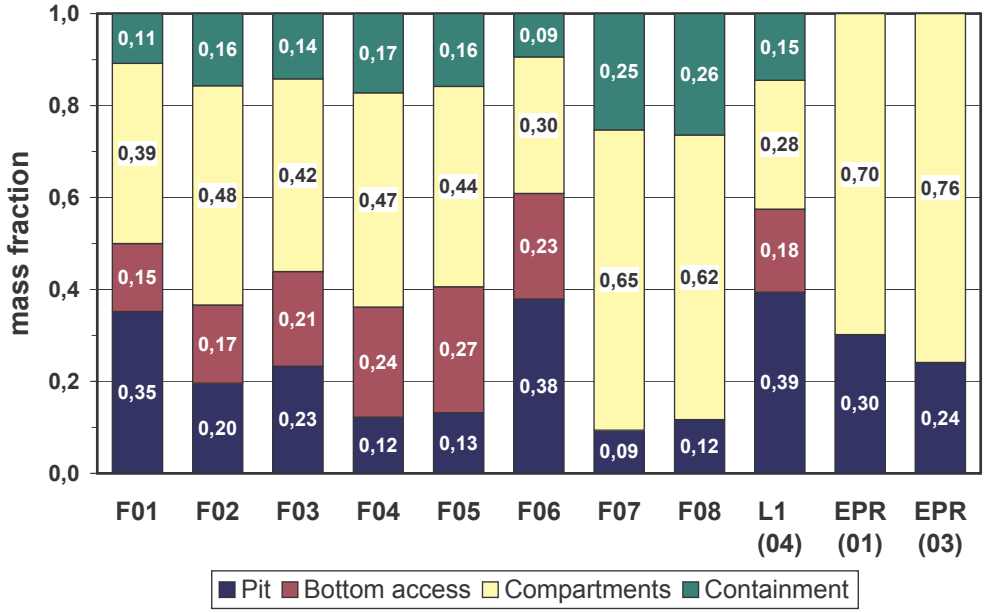

Figure 4: Distribution of liquid fraction in different locations in the 7 cold experiments, the hot L1 test and two cold tests with EPR geometry with conditions similar to F01 and F03

2.2. DISCO-FH experiments

The DISCO-FH facility (which is the DISCO-H facility modified to represent the French geometry) is quite similar to the Cold one except that it is designed for the use of a high temperature corium simulant and encompasses a mock-up of the reactor building. Just as the DISCO-C facility it has also been modified to represent the French 1300 MWe reactor pit geometry (Figure 5). The corium simulant is a mixture of alumina and iron produced by a thermite reaction:

$$119\ \text{mol}\ Fe_3O_4 + 217\ \text{mol}\ FeO + 8\ \text{mol}\ Fe_2O_3 + 511\ \text{mol}\ Al + 37\ \text{mol}\ Al_2O_3 \rightarrow 276\ \text{mol}\ Al_2O_3 + 590\ \text{mol}\ Fe + 33\ \text{mol}\ Al$$

The thermite reaction leads to a heating and additional pressurisation of the RPV. The melt is separated from the cavity by a brass plug. Once the thermite reaction is complete and has reached the plug, this one melts and vaporises, thus releasing the fuel mixture.

Minimum flow area of annulus (between RPV and cavity wall)	0.0110 m^2
Flow area at nozzles	0.0393 m^2
Flow area into containment	0.0114 m^2
Flow area through pit bottom access	0.0060 m^2
Flow area from compartment to containment	0.3226 m^2
Flow area through ventilation duct from pit bottom access	0.0074 m^2

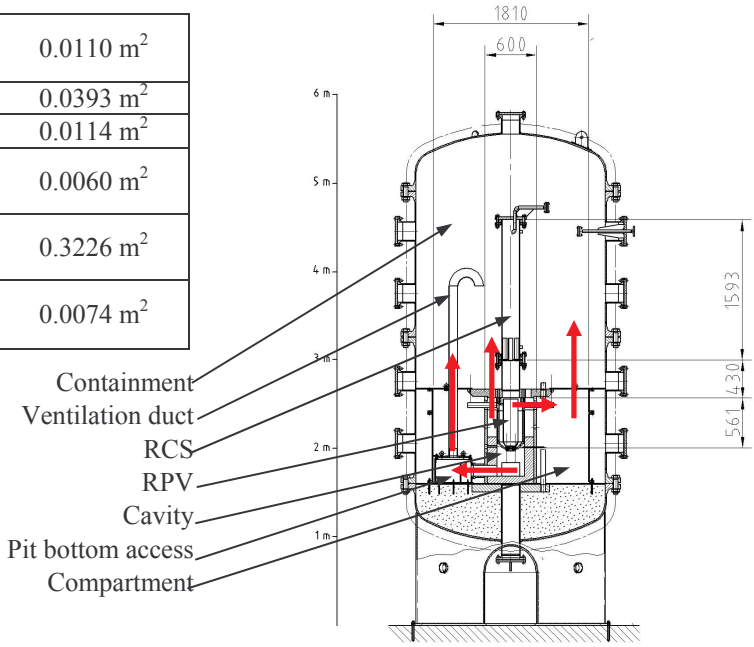

Figure 5: DISCO FH facility showing main paths to the containment and main flow areas

Among this new series, the second test was funded by the EU Commission in the LACOMERA frame (named DISCO-L1 in this frame). Some results have already been provided in the preceding paragraph, some supplementary detail is given hereafter. This experiment has been carried out in an inert environment in order to avoid hydrogen combustion. Then, it focuses on corium dispersion and on containment pressurisation induced by the debris to gas heat exchanges. The specifications of this test were chosen in order to maximize the dispersed fraction of fuel, based on the previous DISCO cold tests (large breach, large pressure). The initial conditions of the test are summarized in Table 2. The breach diameter at rector scale is 1 m. The pressure reached prior to breach opening was 19.1 bar. Note that there was a residual amount of 3% of oxygen in the containment.

The pressure history for the main locations inside the facility are shown in Figure 6. The maximum pressure recorded in the containment is 3.3 bar. The pressure in the lower pit reached 5 bar and 3.9 bar were recorded in the pit bottom access. The thermocouples in the containment show that the average temperature in the containment was around 400 K, 10 s after the beginning of the ejection.

Breach hole diameter	(m)	60 mm
Thermite mass	(kg)	10.64
RPV pressure at failure	(MPa)	1.92
Gas composition in RPV		100% N_2
Gas composition in containment		97 % N_2, 3 %O_2
Containment pressure	(MPa)	0.2
Containment temperature	(K)	303
Melt temperature	(K)	2200 ±100

Table 2: Initial conditions of the LACOMERA DISCO-L1 test

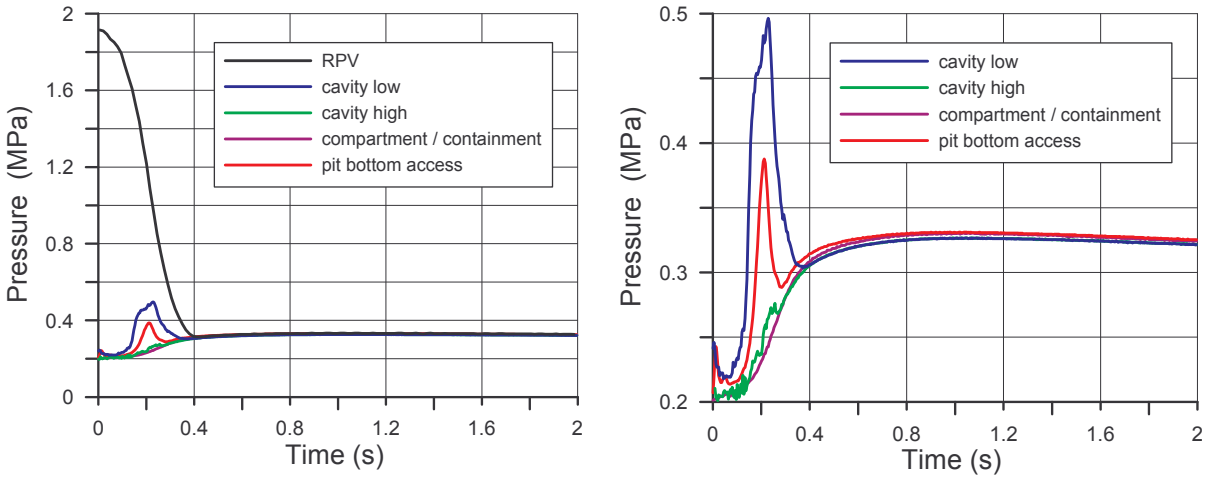

Figure 6: Pressures in the main region of the facility during LACOMERA DISCO-L1 test (right figure is a zoom on cavity and containment pressures)

From the depressurisation rate (Figure 7), we can infer that the transition from single-phase to two-phase flow occurs at approximately 0.090 s. We see that the transition is not as sharp as in cold experiments. Due to the higher density, the transition to two-phase flow occurs later than in water tests. However, as for most of the DISCO-EPR hot tests, the time for transition is also greater than the theoretical time to complete the single-phase flow ejection of the fuel. This might indicate that the opening of the breach is not instantaneous. The linear increase of the depressurisation rate during the single-phase flow gives some consistency to this hypothesis. The picture from Figure 8, right, shows a close view of the breach after the test, where we see that the opening is complete, however.

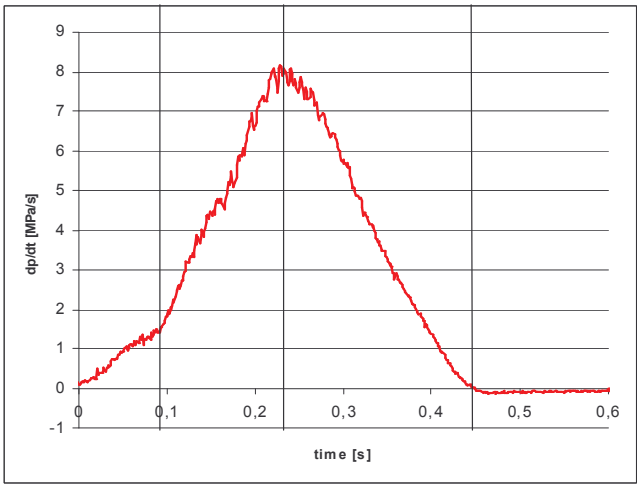

Figure 7: RPV pressure gradient for DISCO-L1

The photos from Figure 9 are taken from video camera recordings. At first, a lot of black smoke is produced in the cavity and escapes starting at t = 40 ms via the compartment into the containment. The origin of the smoke is not clear. Post-test chemical analyses of the dust indicate that most of it comes from the vaporisation of the brass plug. Figure 9, left, shows that at time t = 140 ms some droplets are co-ejected with the black smoke from the compartment to the containment. At t = 180 ms, the video camera at the top of the dome looking downward shows the beginning of melt dispersion into the containment via the direct exit of the pit. The right picture of Figure 9 shows, at t = 340 ms, the melt particle flow into the compartment.

Figure 8: Left : View of the lower head vessel with homogeneous crust from below; Right : View of the breach after the test with some brass around it

All the surface of the cavity was found covered by a thin film of solidified melt (Figure 8, left) and 60.6% of the initial mass of melt was ejected out of the cavity: 14.5% in the containment, 28% in the compartment and 18.1% in the pit bottom access (see Figure 4).

Figure 9: Photos from camera recording during test DISCO-L1. Left : camera looking inside the containment, just above the compartment, middle : camera looking downward above the RPV, right : endoscope looking in the compartment

The sieve analysis (Figure 10) showed that the particles were larger in the compartment (1.76 mm mean mass diameter) than in the containment (0.44 mm on the wall and 0.71 mm on the dome). Interpretation of this result is difficult, because of the tortuous paths covered by the corium simulant and we can only give here some hypotheses. Small particles are entrained under the pressure gradient and should go in both locations according to the section areas. This is what is obtained in water test, where the drops are very small. Large particles might be produced in different ways. Particularly, they might come from the liquid film along the structures that flows from the cavity into the compartment. A large-scale fragmentation might then occur inside the compartment.

A gas analysis was also performed at several instants of the transient and in different locations. Interestingly, it showed some small hydrogen production and the existence of CO and CO_2 as usual products of melt concrete interaction. Because of the small amount produced, it is not believed however that this production has an important impact on the overall transient.

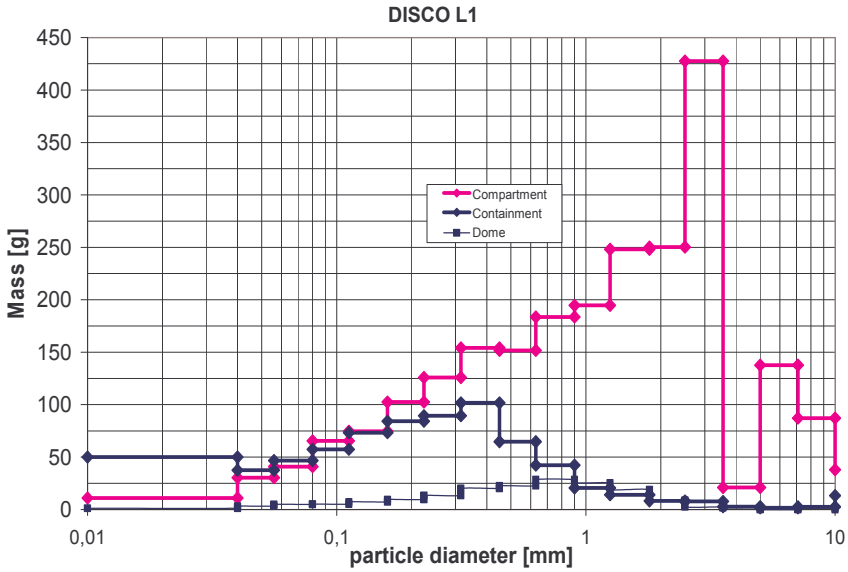

Figure 10: Post-test particle size mass distribution

3. MODELING PROGRAM

The modeling analysis has been performed using the CFD codes AFDM and MC3D. The AFDM code has the capabilities to treat all processes involved from dispersion to combustion and was used to model the whole phenomena occurring during DCH. MC3D has been used to take benefit from its enhanced capabilities for the fuel treatment, with a detailed interpretation of the fuel flow features.

3.1. Analysis with AFDM

3.1.1 The AFDM code

The code AFDM was previously used to recalculate DCH thermite experiments at low system pressures in 1:10 and 1:18 scale. AFDM (Bohl, 1992) is a fluid dynamics code of the SIMMER family of codes which treats transient compressible multiphase flow for three components which are here corium or its simulant, water, and a mixture of gases and vapors. The recalculations DISCO series in EPR geometry was presented at the last NURETH-10 conference (Wilhelm, 2003). The paper also contains a description of major models added to the code for DCH phenomena. Different to the previous presentation of AFDM results on DCH experiments, the code technology as well as the set-up of input data set has been improved so that blind pre-test calculations always preceded the experiments. This contribution is limited to show calculations in P'4 geometry.

3.1.2 Calculation of new DISCO-Cold tests

The calculation of the series of DISCO cold experiments was done first. It was particularly difficult to model the partially 3D geometry of the French reactors in 2D. However, after only a few iterations, the geometrical model was maintained for the rest of the calculations. Fig.11 shows the code model for the two experimental series, hot and cold. It is in 2D cylindrical co-ordinates. The centerline is on the left vertical boundary. The gray shaded areas show cells that are partly filled with structure. The model was verified on the cold series. It stayed unchanged once the different coefficients of fluid-structure momentum transfer were established, and the parameters of the heat exchange model for the film contact with the wall were set. For the pre-test calculation of the first hot experiment, merely the in-vessel details had to be added to model the way that steam is introduced into the pressure vessel of the experiment.

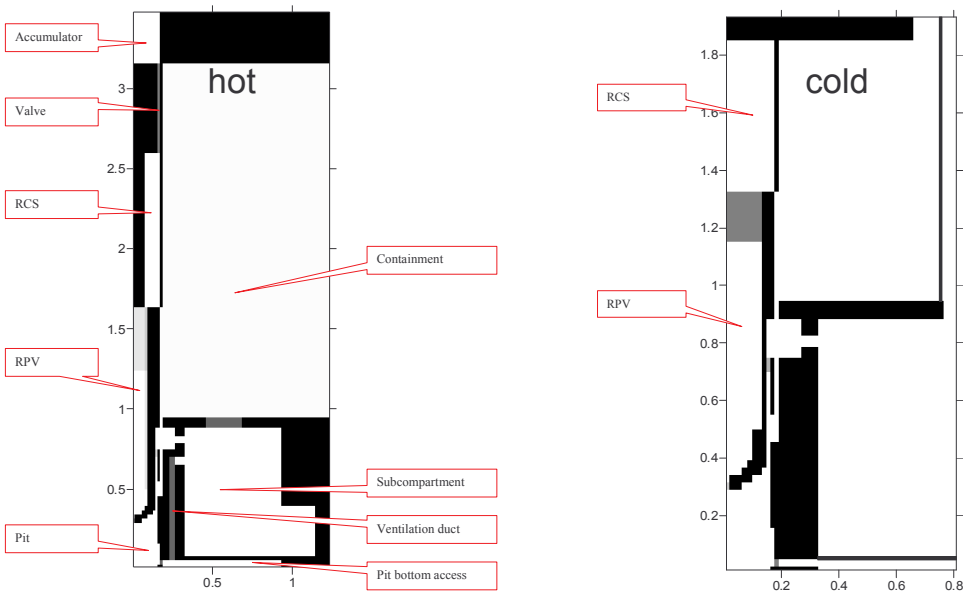

Figure 11: AFDM model of P'4 reactor geometry

Figure 12, left, shows the comparison between measured and AFDM pre-calculated pressures in the reactor pressure vessel and the reactor pit. With respect to future prototypic conditions, the pretest calculations show already satisfactory results. However, as for flow details, the present geometrical model is too coarse to reproduce all measured quantities. Despite of this, the grid which has been set up to resolve the most important flow paths, has not been refined. Indeed, a refinement would introduce possible local peaks of thermal and chemical interaction that may not exist in thermal experiments. The experience from a thorough investigation of the Sandia National Laboratory experiments (Wilhelm, 2001) supports this engineering judgment.

The present cold DISCO series is marked by a large distance between the breach and the pit bottom. From Figure 3, in the experiment F06, at 7 ms, it is not clear that just after breach opening a solid single-phase liquid jet hits the pit bottom. However, the pressure transducer just below the breach indicates this. In the calculation, the liquid jet diffuses to a certain extent before hitting the bottom. Figure 12, right, shows a comparison of measured and calculated pressures for F06, where the pit pressure is taken at the bottom center. The code pit pressure value is the sum of the cell static pressure and the dynamic pressure of the liquid jet. It reaches a maximum of 5.7 bar at 16 ms, while the experiment shows pressures between 10 and 11 bar. This code deficiency is judged unimportant because, first, the thermite will leave the breach as a two-phase jet, and second, because the extrapolation to the reactor will have to account for even more complicated flows through the breach. There, uncertainties with respect to energy transfers dominate the discussion.

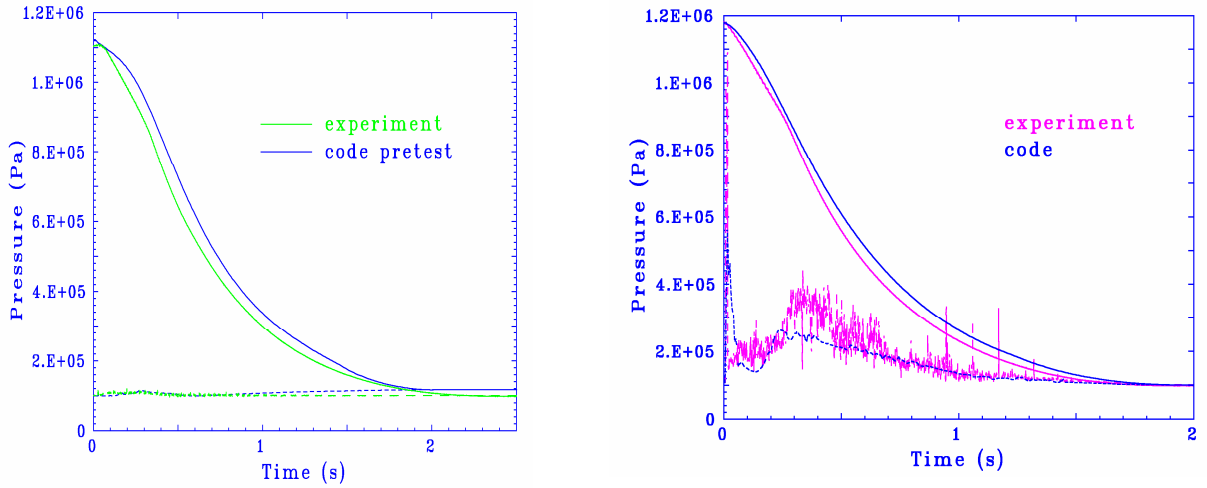

Figure 12: Left : Pressures of F01, solid lines = pressure vessel, dotted lines = pit; Right : Pressures of F06, solid lines = pressure vessel, dotted lines = pit bottom

The large pit volume has a second, more important effect on the fluid flow. Figure 13 shows the inventory changes of the pressure vessel, the subcompartments, and the containment. If the pressure vessel would directly discharge into the containment, the two curves would overlap. The time shift of Figure 13 shows the average time that the water stays in the cavity. It is about 420 ms which is more than 60% longer than in the cavity of the EPR. The figure shows also the time interval during which the experimental observation showed water exiting into the containment. The coincidence with the calculation is an important verification of the validity of the code model. The long residence time of the liquid in the reactor pit will favor a long coexistence of corium and steam which has been called coherence in the American literature.

The isothermal water experiment concentrates on the fluid dynamics. The code has to calculate the proper redistribution of water masses into the different volumes of the experiment. The results depend mainly on the geometrical model and the entrainment and entrapment correlations of the code. These correlations have been left unchanged since the first series of DISCO calculations in EPR geometry in the year 2000. Figure 14 shows the comparison between measured and calculated dispersed mass fractions of all six experiments. Points located on the diagonal show calculations that match measured dispersed mass fraction perfectly. The figure shows that most of the calculated mass fractions lie within an error band of ±30% of the measured values. However, the mass fractions of the pit bottom access show the largest deviations. This can be explained by the difficulty to project a single door onto a two-dimensional model. The main parameters of the tests are listed in the upper left corner of the figure, where M = water volume in liters, D = breach diameters in mm, and P = initial pressures in MPa.

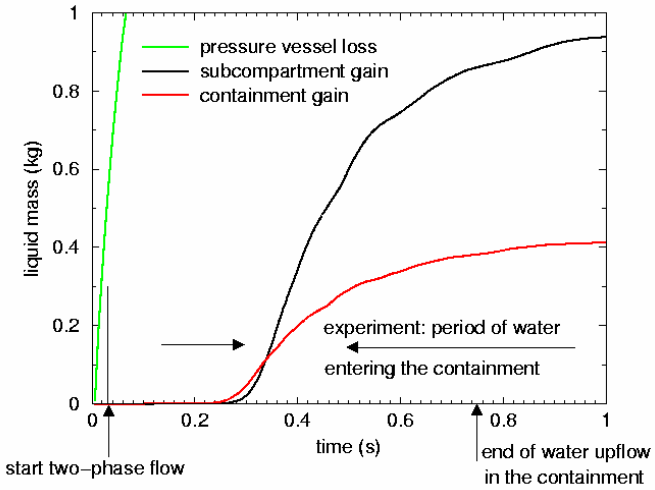

Figure 13 : Water mass balance for the pit of F01

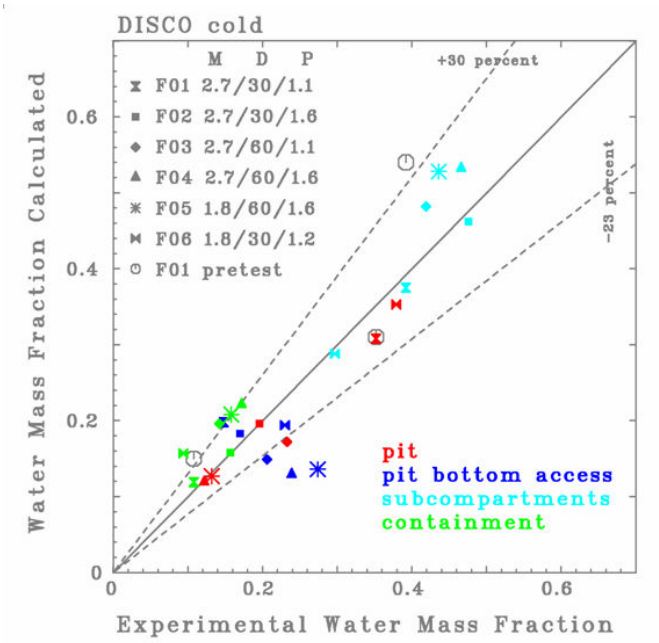

Figure 14 : Comparison of measured and AFDM dispersed mass fractions

3.1.3 Calculations of hot DISCO tests

All DISCO experiments have been pre-calculated. Figure 15, shows the comparison between measured and calculated pressures of the hot DISCO test L1 previously described. The experiment is characterized by a lack of oxygen and steam. In prototypic conditions, the presence of these gases would add to the energetics of the system. The present experiment identifies the thermal part of the dispersion. Only thermal energy is flowing from the hot thermite to the nitrogen. The thermite experiment was planned to start at a vessel pressure of $1.6 * 10^6$ Pa, however, due to the thermal interactions before breach opening bigger than expected, the vessel pressure was $1.9 * 10^6$ Pa. The pressure vessel is filled with nitrogen and then the thermite is ignited. This process is being modeled by starting the calculation prior to breach opening, and letting the nitrogen being heated up by the liquid thermite. The thermite reaction is not modeled. After breach opening at time zero, thermite is flowing into the pit filled with nitrogen. In the breach, the jet is already laden with a small amount of tiny bubbles. The thermite is dispersed into the pit volume, and a liquid film builds up at the pit bottom. When the two-phase thermite jet fades out after 150 ms, nitrogen gas is leaving the vessel at increasing velocities. The velocities are high enough to entrain a part of the thermite out of the film. The hot droplets heat up the gas. The hot gas which exits into the subcompartments and the reactor containment increases the containment pressure. The pressure rise in the containment is only 1.3 bar.

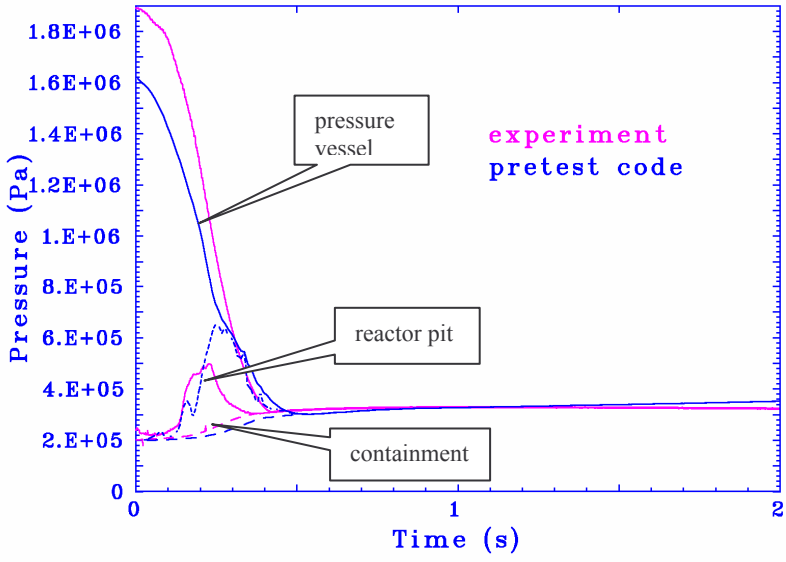

Figure 15: Comparison between measured and AFDM pressures of experiment L1

3.2. Interpretation with MC3D

MC3D is being developed at the IRSN and CEA mainly for the description of the Fuel Coolant Interaction. However, the capabilities of the code to treat most of the phenomena occurring during DCH have been demonstrated by calculations of some of the EPR-DISCO tests (Meignen, 2004). Currently, the code is unable to calculate the combustion. All other aspects, including oxidation can be treated at least parametrically. Up to now, the use of the code is however restricted to experiments without oxidation since this one is always accompanied by a combustion.
MC3D is a semi-implicit Eulerian multi-fluid thermal-hydraulic code built on a concept of "application", consisting of prescribed sets of balances and exchange laws between fields. For the DCH calculations, we use the premixing "application" of MC3D, version 3.4.03, which contains:

- 6 material fields with 3 devoted to the fuel description:
  - water
  - steam
  - non-condensable gas
  - continuous fuel
  - discontinuous fuel (drops)
  - fuel fragments
- 4 velocity and thermal fields
  - water + fuel fragments
  - gas
  - continuous fuel
  - fuel drops

For the purpose of DCH, water and fragments are not used. The fragment field would be useful to describe two fields for the dispersed fuel, but this requires some modifications that should be done in the future. Note also that in the next version of MC3D, V3.5, an indefinite number of non condensable gases will be available. The continuous field is modeled with an original VOF-like[2] volume tracking method. The use of the VOF method is illustrated in Figure 17 where a visualization of the flow calculated by the code for a DISCO test with Wood's metal is provided, at the time of the transition from single to two-phase flow at the breach. The continuous fuel is here pictured in red. Fuel drops are generated from this continuous field by a fragmentation mechanism based on an adaptation of the Kelvin-Helmholtz instability model. The inverse process, i.e. coalescence can also happen in two cases: high volume fraction and impact on a wall. The fragments, when used, are coming from the secondary fragmentation, i.e. fragmentation of the drops.

Due to the uncertainties concerning the 3-D representation in 2-D geometry, we have limited up to now our calculations to 2-D symmetric tests, i.e. the DISCO-cold tests with restricted symmetric geometry F07 and F08. The grid used for the calculations is shown in Figure 18 for a restricted part around the pit. Fuel is simulated by water and the conditions are in Table 1. Figure 19 shows a comparison of the pressures in the vessel and the cavity (at the jet impact location), together with a comparison of the repartition of fuel in the containment and compartment. As for the EPR tests with Wood's metal, the comparison is largely satisfying. A visualization of the calculated flow is provided in Figure 20 and compared to the experiment in Figure 21. Here, due to the large breach, the flow is very rapidly in a two-phase pattern (0.007 s.). The visualization in the experiment is unclear due to the fog created probably by the design of the plug once it is open. We can however distinguish a single-phase jet flowing downward up to approximately 0,0065 s. At 0.007, the pattern seems different, indicating a transition towards the two-phase flow. As for the calculation, the transition occurs at the time the jet reaches the bottom. Note also that, in contrast with the calculations of tests with Wood's metal (Figure 17), there is some noticeable fragmentation along the jet prior to the transition time. At t = 0.05, the location of the drops in the visualization of the calculation is consistent with the picture taken from the experiment where the density of the fog seems more important in the upper part of the pit. These drops are calculated to be very small, of the order of 50 µm. From the pictures, it is not possible to distinguish the drops themselves, giving the impression of a fog flow. In this respect, there is also a

[2] Volume Of Fluid

clear difference with the cases with high density liquid as with Wood's metal or corium. The case of the corium simulant used in DISCO-Hot tests should be in-between this two extreme behaviors.
The end of two-phase flow in the calculation is not very clear. We should however say that two-phase flow is almost accomplished at approximately 0.12 s. This compares well with the Table 1 (see F06). The ejection out of the cavity is seen to be nearly complete and finished at t = 0.2 s.

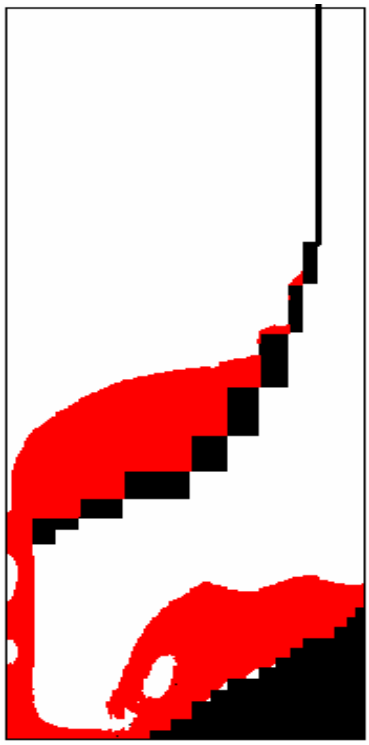

Figure 17: Illustration of the VOF model for the continuous fuel field, showing the time of transition from single-phase to two phase flow in a DISCO test with Wood's metal (EPR geometry)

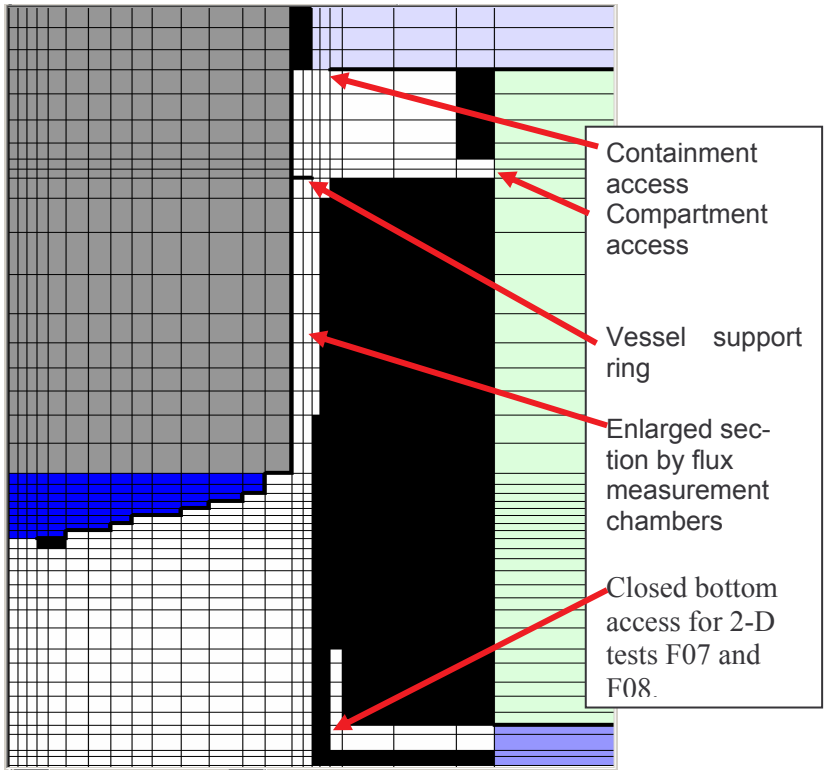

Figure 18: Mesh used for cold test: zoom around the pit showing the main flow path for F07 and F08, dark blue: initial water location, other colors simply indicate different parts of the facility

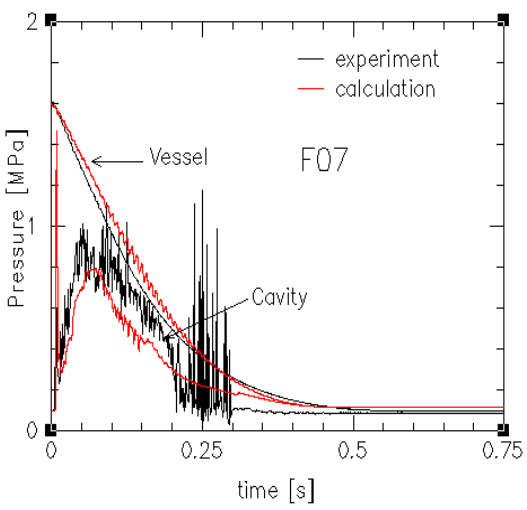

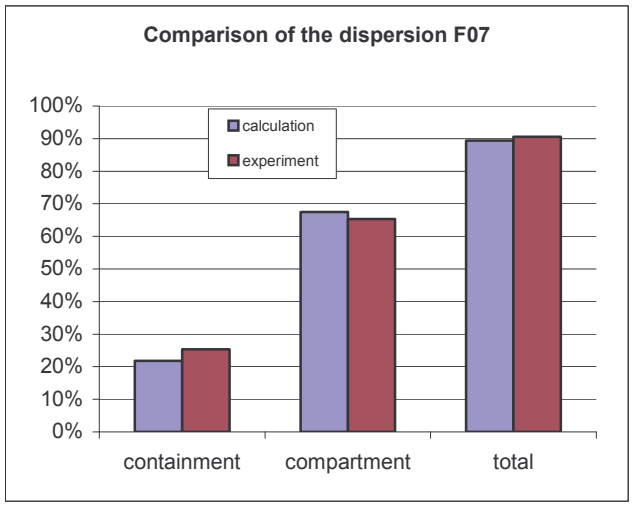

Figure 19: Left : calculated and experimental pressures in the vessel and in the cavity for test F07; right: comparison of the dispersion of the fuel

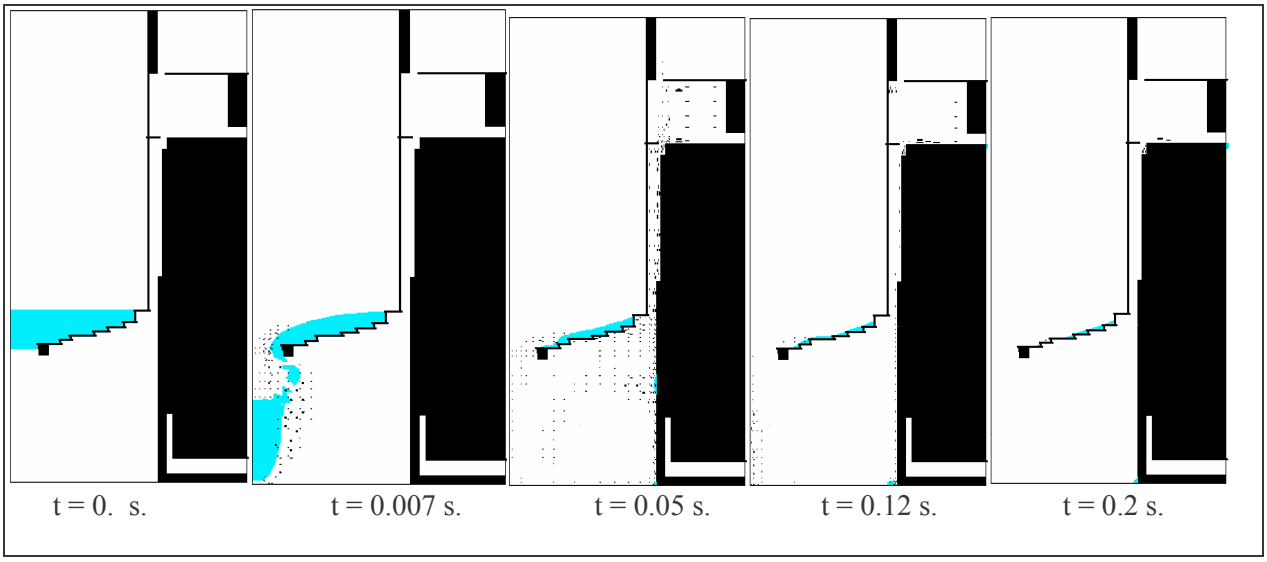

Figure 20: Visualization of the fuel flow pattern at the time of two-phase transition in DISCO F07, blue : continuous fuel field, black dot : fuel drops

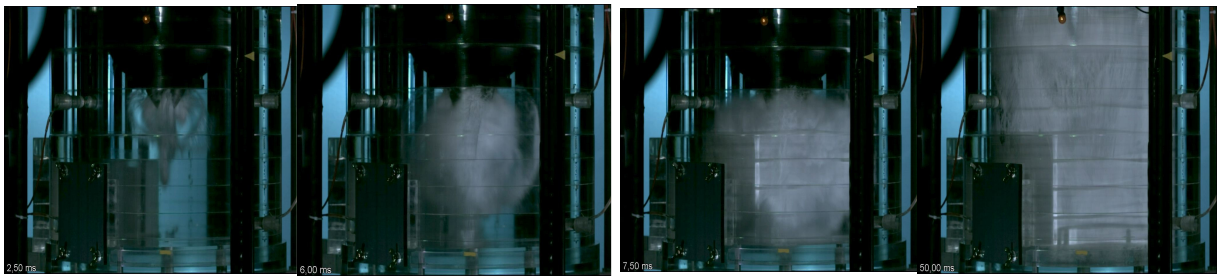

Figure 21: Visualization of the flow in the experiment F07

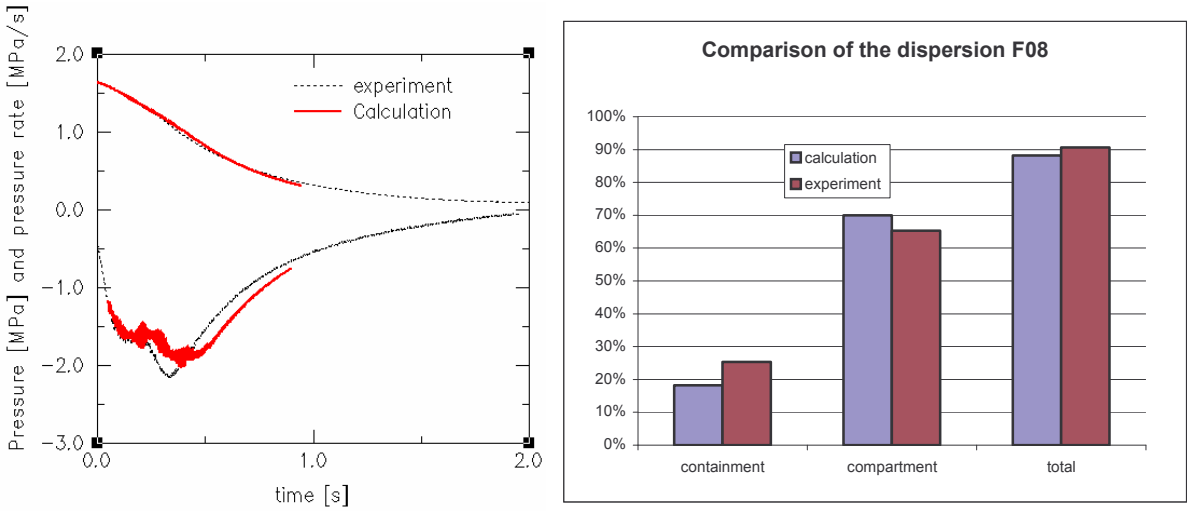

Figure 22: Left : Pressure and depressurization rate for test F08, Right: distribution of water

Similar trends are obtained with the calculation of experiment F08 (Figure 22) with a longer time scale due to the reduction of the breach diameter. The two-phase flow starts a little before 20 ms, as expected from the experiment. The end of this two-phase flow in the calculation is here again difficult to establish from visualizations (not shown here) but it can be estimated at approximately 0.4 s. As for F07, this time corresponds approximately to the change in slope of the depressurization rate. The dispersion is very similar to F07.

4. CONCLUSIONS, FUTURE WORK

We have presented the status of an ambitious program devoted to the DCH issue in order to clarify the involved phenomena, improve modeling and predictions and finally allow extrapolations to reactor situations. This work is accomplished under a French-German collaboration frame between FZK and IRSN and extends the work done for EPR reactors. The geometry used for this program is representative of French P'4 reactor at 1:16 scale. The experimental part is done within the DISCO Cold and Hot facilities. Except the geometry, all other aspects, from the simulant to the conduct of the experiments, are similar to those of the previous DISCO-EPR tests. The cold part of the experimental program is done with water for the first 10 tests, and with a metal for the 4 last ones. The water test part is completed. Two hot tests have been performed with one funded by the EU Commission, with the LACOMERA frame. This test is presented in details. First results indicate that, compared with EPR, the P'4 geometry leads to a smaller dispersion in the containment, mainly because of the pit height and of the presence of the pit bottom access. The impact of the different geometry regarding to the heat transfer, the oxidation and combustion will be investigated with the help of the next 3 tests to be performed.

Due to the complicated geometry used for the experiments, the work of interpretation and modeling is very challenging. It is seen that the 2-D code AFDM can manage with the 3-D aspects of the geometry in a satisfying way for both the cold and hot cases. The use of MC3D for interpretation of DCH is far more recent. The emphasize is currently put on dynamical aspects. Encouraging results are obtained.

In the light of the present demonstrated modeling capabilities, it seems rather clear that the ultimate task for modeling and extrapolating to reactor situations is, once again, related to the chemical aspects, i.e. oxidation and combustion.

References

de Bertodano, M. L., Becker, A., Sharon, A., Schnider, R., 1996, DCH Dispersal and Entrainment Experiment in a Scaled Annular Cavity, *Nuclear Engineering and Design*, **164**, pp.271-285

Blanchat, T.K., Pilch, M.M., Allen, M.D., 1997, Experiments to Investigate Direct Containment Heating Phenomena with Scaled Models of Calvert Cliffs Nuclear Power Plant, NUREG/CR-6469, SAND96-2289, Sandia Laboratories, Albuquerque, N.M.

Bohl, W.R., Wilhelm, D., 1992, The Advanced Fluid Dynamics Model Program: Scope and Accomplishment, *Nuclear Technology*, **99**, pp.309-317

Cranga, M., Giordano, P., Passalacqua, R., Caroli, C., Walle, L., 2003, ASTEC RUPUICUV code – Version 1.2 Ex-vessel corium discharge and corium entrainment to containment, ASTEC-V1/DOC/03-19

Kim, S.B., Park, R.J., Kim, H.D., Chevall, C., and Petit, M., 1999, Reactor Cavity Debris Dispersal Experiment with Simulant at Intermediate System Pressure, SMiRT15 Post Conference Seminar on Containment of Nuclear Reactors, Seoul, Korea, August 23-24

Meignen, R., Dupas, Chaumont B., 2003, First evaluations of ex-vessel fuel coolant interaction with MC3D, NURETH-10, Seoul, Korea, October 5-9

Meignen, R., Plet D., Caroli C., Wilhelm D., 2004, Meyer L., IRSN-FZK cooperation on Direct Containment Heating. Experimental and modeling research, CSARP 2004, May 3-4, Arlington,USA

Meignen, R., Status of the qualification program of the Multiphase Flow code MC3D, ICAPP 2005, Seoul, May 2005

Meyer, L., Gargallo, M., 2003, Low Pressure Corium Dispersion Experiments with Simulant Fluids in a Scaled Annular Cavity, Nuclear Technology, 141, pp.257-274

Meyer, L., Albrecht, G., Wilhelm, D., 2004, Direct Containment Heating Investigations for European Pressurized Water Reactors, 6th International Conference on Nuclear Thermal Hydraulics, Operations and Safety (NUTHOS-6), Nara, Japan, October 4-8

Pilch, M.M. and Allen, M.D., 1996, Closure of the direct containment heating issue for Zion, *Nuclear Engineering and Design*, **164**, Issue1-3 , pp.37-60

Wilhelm, D. 2001, Analysis of a thermite experiment to study low pressure corium dispersion. Wissenschaftliche Berichte, FZKA-6602

Wilhelm, D., 2003, Recalculation of Corium Dispersion Experiments at Low System Pressure, NURETH-10, Seoul, Korea, October 5-9